Materials Research. 2013; 16(6): 1315-1324
DOI: 10.1590/S1516-14392013005000115

Environmentally Friendly Sol–gel-based Anticorrosive Coatings on Aluminum Alloy 2024

***Giancarlo Richard Salazar-Banda*[a]*, *Katlin Ivon Barrios Eguiluz*[a], *Artur Jesus Motheo*[b], *Sergio Antonio Spinola Machado*[c]**

[a]*Laboratório de Eletroquímica e Nanotecnologia, Programa de Pós-graduação em Engenharia de Processos, Instituto de Tecnologia e Pesquisa, Universidade Tiradentes – Unit, CEP 49032-490, Aracaju, SE, Brazil*
[b]*Grupo de Eletroquímica Interfacial, Instituto de Química de São Carlos – IQSC, Universidade de São Paulo – USP, CP 780, CEP 13566-590, São Carlos, SP, Brazil*
[c]*Grupo de Materiais Eletroquímicos e Métodos Eletroanalíticos, IQSC, Universidade de São Paulo – USP, CP 780, CEP 13566-590, São Carlos, SP, Brazil*

Received: March 26, 2013; Revised: May 29, 2013

Chromate coatings used as corrosion protection technologies for aluminum alloys are environmentally harmful and extremely toxic. This paper presents an investigation on the deposition of environmentally friendly cerium oxide-based anticorrosive coatings on aluminum alloy 2024 substrates by the sol–gel method. The influence of the calcination temperature on both the microstructural characteristics and the electrochemical corrosion performance was tested using scanning electron microscopy, X-ray diffraction, potentiodynamic polarization and electrochemical impedance spectroscopy (EIS), before and after, periods of immersion in saline corrosive solutions. The ceramic coatings synthesized at 200, 300 and 400 °C showed very resistive behaviors leading to both an efficient passivation of the alloy surfaces and good corrosion protection. This passivation was maintained for 30 days of immersion in saline solutions, as well as, when aggressive electrochemical polarization experiments (until 2.0 V *versus* saturated calomel electrode) were used. Very high resistances for the charge transfer (0.14-0.28 GΩ) and very low current density values (5×10^{-14} -5×10^{-11} A cm^{-2}) were estimated by EIS and potentiodynamic polarization, respectively, for coatings prepared at 200-400 °C. Thus, the coatings prepared in this study by the sol–gel method appear as an efficient treatment for the corrosion protection of aluminum alloys.

Keywords: *Sol–gel growth, cerium oxides, corrosion protection, AA2024-T3, electrochemical impedance spectroscopy*

1. Introduction

The aluminum alloy 2024 (AA2024) is widely used for structural applications in the aerospace industry due to its good combination of high strength, fatigue resistance and low density. Unfortunately, these advantageous mechanical properties are accompanied by poor alloy resistance toward intergranular corrosion and stress corrosion cracking. In fact, the alloying element that is responsible for the localized corrosion susceptibility of the AA2024 alloy is copper[1].

Corrosion protection for AA2024 surfaces is provided by chromate conversion coatings in a first step. However, due to the high toxicity and carcinogenic properties of hexavalent chromium (Cr^{6+})[2], environmentally benign alternatives to chromates are strongly needed.

The corrosion protection behavior of anticorrosion coatings can be active and/or passive. The passive corrosion protection is achieved by deposition of a barrier layer preventing the contact of the material with the corrosive environment[3], for instance, traditional metallic oxide-based coatings commonly provide passive corrosion protection. The active corrosion protection aims at a decrease of the corrosion rate when the main barrier is damaged and corrosive species come in contact with the substrate[3]. Cerium salts using as inhibitors have shown to provide active protection for aluminum alloys against corrosion[4-6] as well as cerium-based coatings prepared by sol–gel method[7]. Corrosion protection is attributed to the formation of cerium oxide or hydroxide films containing Ce^{3+} and Ce^{4+} [8]. Cerium(IV) oxides detected in the coating were believed to arise from oxidation of Ce^{3+} in oxygenated alkaline solutions[9].

Sol–gel technologies excel in the production of thin, scratch-resistant metal oxide coatings for corrosion protection[10]. This method offers some advantages like good adhesion of the coating to metallic surfaces via chemical bonding and also good physical bonding to organic top coats when subsequently applied to the cured sol–gel, cost-effectiveness, low life-cycle environmental impact and simple application procedures easily adaptable within industry[10,11].

*e-mail: gianrsb@gmail.com

Several reports have been published regarding the development of organic-inorganic hybrid silane sol–gel coatings with cerium nitrate as dopant and corrosion inhibitor on aluminum alloys with good performance as corrosion protection systems[12-14]. Furthermore, the deposition of cerium oxide coatings on AA7075-T6 surfaces by sol–gel method at 300 and 400 °C of calcination temperature produced very efficient active barrier against corrosion[7].

Hence, this study presents the development of anticorrosive cerium oxide coatings prepared by the sol–gel method using a broad range of deposition temperatures (100, 200, 300 and 400 °C) on AA2024 substrates. Their microstructural characterization and electrochemical corrosion testing was carried out by scanning electron microscopy (SEM), energy dispersive X-ray spectroscopy (EDX), X-ray diffraction (XRD), potentiodynamic polarization and electrochemical impedance spectroscopy (EIS). The anticorrosive performance of the coatings was tested, showing that the calcination temperature used in the synthesis has considerable influence on the efficiency of the protective coating.

2. Experimental Section

For the preparation of the cerium sol precursors, 4.78 g of ceric ammonium nitrate ($Ce(NH_4)_2(NO_3)_6$ from Mallinckrodt Chemicals, USA, with 99% of purity) were dissolved, in the sequence, in 10 ml of ethanol (Vetec®, Brazil, P.A. 99.5%), 2.5 ml of ultrapure water and 2.5 ml of acetic acid, using the latter as catalyst, (Merck®, Germany, P.A. 99.8%). The estimated final concentration of cerium dioxide (CeO_2) in the sols was 200 g L^{-1}.

The sols obtained were initially dark red and changed in about two hours producing a colorless sol. This phenomenon is explained by the reduction of Ce^{4+} to Ce^{3+} state, as reported by Verma et al.[15], which is related to the presence of alcohol in the initial sol[16], since no color change was observed by these authors in aqueous acidic solutions of ceric ammonium nitrate over a period of several days. The Ce^{4+} is a strong oxidizing agent that can easily oxidize an alcohol to the correspondent aldehyde. In this sense, the redox process between Ce^{4+} and methanol has been previously demonstrated[17], and the oxidation product, formaldehyde, has been identified by trapping techniques[18]. The sol precursors prepared in our study were stirred by sonication in ultrasound (Sonicator Ultrasonic Processor XL) equipment for half an hour previous to their deposition on alloy samples, to avoid the complete reduction of cerium.

The AA2024–T3 samples were cut in the form of disks (2 cm diameter, 1.5 mm thick) proper to place in a cylindrical holder. The alloy samples were polished in wet (in water) silicon carbide sandpapers, in the sequence of 400, 600, 1500 and 2000 mesh. Later, the disk surfaces were polished in a low-rotation polisher, using soft velvet impregnated with diamond powder of 1 μm of diameter and finally they were ultrasonically cleaned in acetone and ultra pure water, in sequence.

AA2024 substrates were coated with sol–gel precursor solutions using a dip-technique at a withdrawal rate of 10 cm min^{-1}. The coated samples were dried at room temperature (≈ 28 °C) for 20 min for both the polymerization of the sol producing a gel on the alloy surfaces and the evaporation of volatile solvents. Subsequently, the samples were subjected to a thermal densification treatment at 100, 200, 300 or 400 °C, for 1 h at the final temperature, in an electric oven using a heating rate of 5 °C min^{-1}. It is worthwhile mentioning that when thermal treatments at higher temperatures (500 and 600 °C) were used, the alloy showed deformations, which were observed by SEM images (images not shown), and consequently, these temperatures are not appropriate for the coatings deposition.

Electrochemical experiments were carried out in a home-made developed one-compartment Pyrex® glass cell provided with three electrodes[7]. Briefly, an adapter was developed for the working AA2024 electrodes that were clamped in firm contact at the side of the cell using of a rubber O-ring leaving an exposed area of 2.0 cm^2, whereas the electrical contact was made through a copper plate at the bottom of the electrodes. The reference electrode was a saturated calomel electrode (SCE) whose potential was tested just before the measurements and all potentials are referred to this system. The auxiliary electrode was a 5-cm^2 (each face) Pt foil.

All measurements were conducted at least in duplicate and within aqueous 3.5% sodium chloride (0.6 mol L^{-1}) solution prepared using water purified by a Milli-Q system from Millipore. The electrochemical tests were performed under deaerated conditions provided by a nitrogen gas bubbler where N_2 (99.998%) was introduced from a compressed gas cylinder for 15 min before each experiment. Alternatively, the solutions were deareated prior to the immersion time tests and subsequently air-exposed during the following days of testing.

Potentiodynamic polarization measurements were done to determine the degree of protection against corrosion provided by the sol–gel coatings and to establish the nature of the inhibition process. Electrochemical data were obtained using an Autolab Model PGSTAT 30 potentiostat/galvanostat coupled to an IBM-PC compatible microcomputer. After open-circuit potential (OCP) measurements (2 h), potentiodynamic scans were performed at a rate of 1 mV s^{-1} from –1.5 to –0.4 V for the bare alloy and, in more aggressive conditions, from –1.5 to 2.0 V for the coated alloy samples.

Electrochemical impedance spectroscopy studies were carried out in order to assess the anti-corrosion performance of the sol–gel films deposited on AA2024 for different times of immersion in 3.5% NaCl solution. The impedance measurements were tested at OCP applying 10 mV sinusoidal perturbations in the frequency range from 100 kHz to 10 mHz. At least two samples were measured for each coating to ensure reproducibility.

The microstructure of the sol–gel coatings before and after immersion in saline solutions was studied by a SEM system LEO Mod. 440 with a silicon-lithium detector, a Be window, and applying 113 eV. EDX analyses were obtained with the same equipment. X-ray diffractograms of the coatings were obtained in a universal diffractometer Carl Zeiss-Jena, URD–6, operating with Cu Kα radiation (λ = 0.15406 nm) generated at 50 kV and 100 mA. Scans

were carried out as continuous scan at grazing incident angle at 1° min^{-1} for 2θ values from 10 to 100°.

3. Results and Discussion

3.1. *Physical characterization*

Figure 1 shows XRD patterns obtained for the deposits prepared using different calcination temperatures. These patterns reveal the presence of crystalline cerium dioxide (CeO_2) deposits (Joint Committee of Power Diffraction Standards-JCPDS #43-1002) with characteristic peaks in the 2θ values of 28.6, 33.0, 47.5, 56.3, 69.4 and 88.4° corresponding to the reflection planes of the cerianite (ceria) structure (111), (200), (222), (311), (400) and (422), respectively. This preferential deposition is expected for the sol–gel method and is in agreement with previous reports that observed the same 2θ values for crystalline CeO_2 coatings prepared by the sol–gel method, also using ammonium cerium nitrate as precursor[7,19]. Note that the ammonium cerium nitrate used in our study is the cheapest cerium precursor for sol–gel applications. The signals associated to the aluminum metal from the substrate (JCPDS: 04-0787) are also observed in Figure 1.

The presence of crystalline CeO_2 is obvious in the coatings synthesized at 200, 300 and 400 °C of calcination temperature with well-defined peaks observed in the diffractogram patterns of Figure 1. The peaks, corresponding to cerium dioxide, are apparently higher for the coatings deposited at 300 and 400 °C and the Al/CeO_2 ratio is higher for the coating deposited at 200 °C. It suggests that the latter coating is formed probably by a mixture of crystalline and amorphous phases and that the higher the calcination temperature the higher the portion of crystalline deposit in the coating.

On the other hand, the coating deposited using 100 °C seems to be mainly formed by amorphous cerium oxide phases which could avoid the X-ray radiation to reach the substrate surface and consequently could mask the Al signals in the pattern. Thus, higher temperatures are needed for the formation of crystalline deposits.

The same crystalline composition of the coatings synthesized at 300 and 400 °C was observed in a previous report that used similar experimental conditions to prepare cerium-based coatings on AA7075 substrates[7]. In that report, X-ray photoelectron spectroscopy measurements showed that although crystalline CeO_2 was identified by XRD experiments, the sol–gel deposits present small quantities of Ce_2O_3 and cerium hydroxides, most likely in the non-crystalline form.

On the other hand, the four SEM images (5000×) shown in Figure 2 (A, B, C and D) revealed that the cerium oxides were homogeneously deposited over the alloy surfaces but with different aspects. The coatings deposited at 300 and 400 °C (Figure 2C and 2D, respectively) appear as compact micro-cracked films of ceramic characteristic, while the coatings deposited at 100 and 200 °C (Figure 2A and 2B, respectively) show a non uniform surface with some agglomerates. The uneven deposition of the coatings is related to the different crystalline structure observed by XRD measurements, where higher calcination temperatures produce more crystalline compositions which are also similar

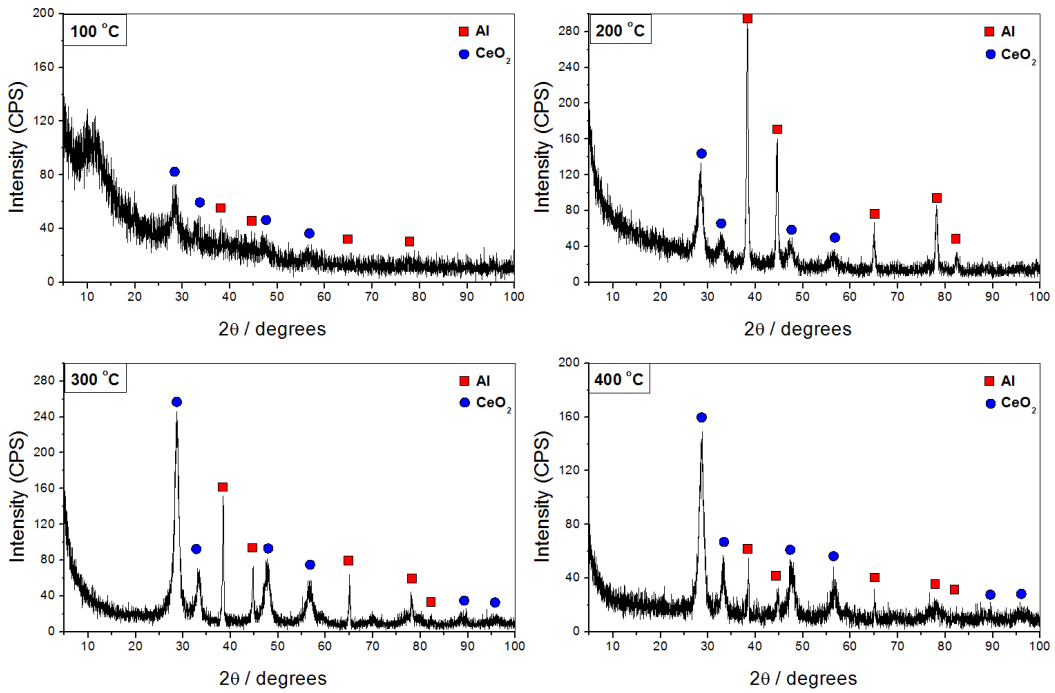

Figure 1. Grazing incident angle X-ray diffraction patterns for the cerium-based coatings prepared at 100, 200, 300 and 400 ºC.

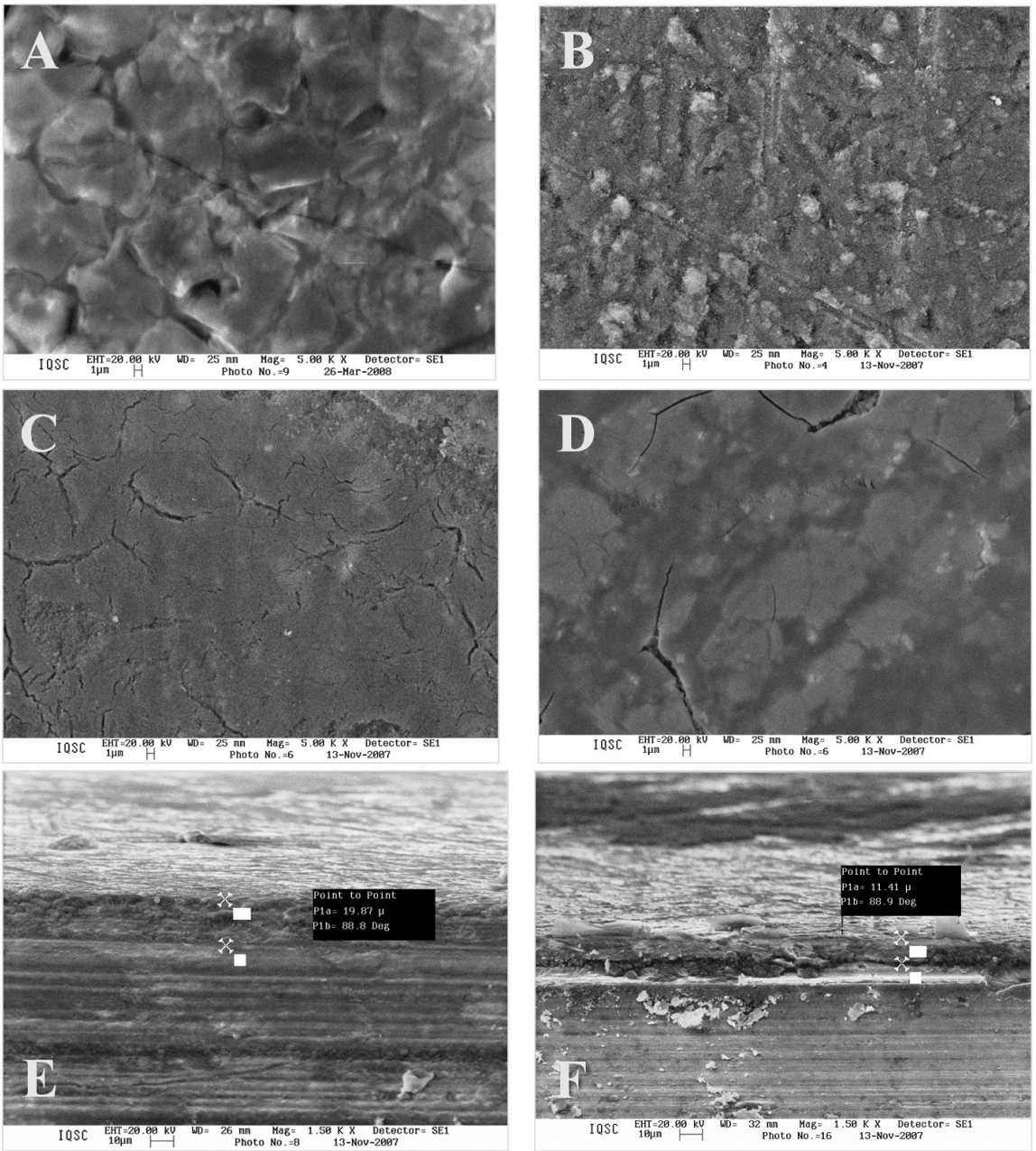

Figure 2. SEM images (5000×) recorded for the cerium-based coatings just prepared at 100 (A), 200 (B), 300 (C) and 400 ºC (D). Cross-section SEM images (1500×) recorded for the Al alloy protected with cerium-based coatings prepared at 200 (E) and 300 ºC (F).

to the common 'cracked mud' aspect of crystalline sol–gel based coatings prepared using thermal decomposition[20-22].

The thickness of the coatings were determined using cross-section SEM images, as shown in the two micrographs of Figure 2E and 2F for coatings synthesized at 200 and 300 °C, respectively, which are representative of all the coatings prepared in this study. The mean thickness of all the coatings (n=4 for each temperature), is 15 µm ± 1 µm. This value of thickness is comparable (10-12 µm) to the ones measured for anti-corrosion organic-inorganic hybrid silane sol–gel coatings prepared using N-[3-(Trimethoxysily) propyl]ethylenediamine, 3-aminopropyltriethoxy-silane, 3-glycidoxypropyltrimethoxysilane, and 3-methacryloxypropyl-trimethoxysilane on aluminum and iron plates[23]. However, the thicknesses obtained for the deposited coatings, by sol–gel, were lower than both the thickness obtained using aminosilane-epoxy deposited on AA2024-T3 and epoxysilane-epoxy on AA7075-T6 (30-50 µm)[24] and to the ceramer coatings developed using soybean oil as the organic phase with mixtures of titanium

isopropoxide and zirconium propoxide as the inorganic phase (45-95 µm)[25]. The thickness was also lower than the 30 µm observed for an Al_2O_3 protective coating synthesized by direct sol–gel process on magnesium alloy AZ31[26].

It is worthwhile mentioning that in the 'U.S. Military Specification: Anodic Coatings for Aluminum and Aluminum Alloys'[27], thickness in the range from 0.0005 to 0.0045 in (12.7-114.3 µm) are recommended for type III coatings (resulting of treating aluminum and aluminum alloys electrolytically to produce a uniform anodic coating on the metal surface) and in the range from 0.00002 to 0.0007 (0.51-17.8 µm) for type I and IB coatings (resulting of treating aluminum and aluminum alloys electrolytically in a bath containing chromic acid to produce a uniform anodic coating on the metal surface). Notably, the thicknesses of the sol–gel-based coatings prepared in this study are inside both of ranges described above.

Furthermore, the thin cracks formed in response to stresses in the gel films on a solid surface and observed on the deposits prepared at 300 and 400 °C are not apparently very deep, as observed in the cross-section SEM image taken for the coating prepared at 300 °C (Figure 2F). This fact is important because it avoids the contact between the metallic substrate and the environment.

EDX analyses (figures not shown) confirmed the presence of cerium in the coatings and suggested the formation of cerium oxides due to the increase in the oxygen content (40-53%) on the AA2024 substrates after the deposition of the sol–gel coatings. These outcomes match with the XRD results confirming the formation of cerium oxides.

3.2. *Corrosion behavior*

The potentiodynamic polarization curves in Figure 3 show that the corrosive behavior of the alloys with coatings prepared at 200, 300 and 400 °C of calcination temperature (curves indicated inside the figure) is very different to the observed for the alloy without protective coating (identified as 'bare' in Figure 3). The protected alloys display very resistive behaviors with very low current density values (in the range from 5×10^{-14} to 5×10^{-11} A cm^{-2}), which are typical of non-conductive materials, like the ceramic coatings prepared here. Additionally, not well-resolved corrosion potential regions are depicted with the form of plateaus in the polarization curves, without any physical sense. This occurs probably because the current density values are very close to the detection limit of the potentiostat. Note that the polarization curves of the alloys with cerium oxide coatings were carried out in a very wide range of potentials, between –1.4 and 2.0 V *versus* SCE (3.4 V), which is higher than the commonly used range of about 1.0 V (0.5 V before and 0.5 V after the corrosion potential) as observed for the bare alloy.

The protective coatings prepared at 200, 300 and 400 °C are very efficient in the passivation and protection of the alloy surfaces, since they displayed very small current density values in the polarization curves.

In contrast, the alloy with coating prepared at 100 °C (curve indicated inside Figure 3) presents a similar behavior to the one observed at the bare alloy. However, a decrease in the

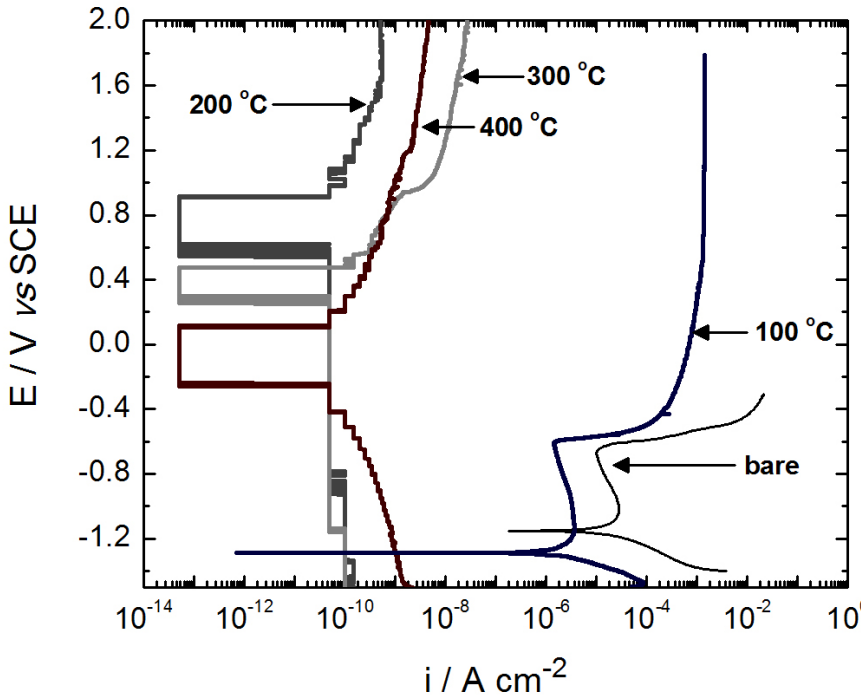

Figure 3. Polarization curves carried out from –1.5 to –0.4 V on the bare AA2024 and carried out from –1.5 to 2.0 V on the alloys containing the cerium oxide-based coatings prepared at 100, 200, 300 °C and 400 °C. Electrolytes used were 3.5% NaCl solutions.

corrosion current density of one order of magnitude is observed in the protected alloy, that is important for the corrosion protection of the alloy and is very similar to that presented by electropolymerized polyaniline coatings deposited on AA2024[28,29], and on AA3004[30]. Besides, a negative change in the corrosion potential of 140 mV is also observed. This small improvement could be due to the presence of other cerium compounds in the coating that did not form oxides, as observed in the XRD patterns of Figure 1; however these compounds in the coating still prevents the surface against corrosive attack in solutions containing chloride ions.

The SEM images displayed in Figure 4 were taken after making the potentiodynamic polarization experiments from Figure 3. The SEM images of the protected alloy surfaces seem similar than the SEM images taken for the as-prepared coating samples (Figure 2), mainly for the coatings prepared at 200, 300 and 400 °C. These coatings were efficient for corrosion protection even when high potentials (2 V *versus* SCE) are used. The protective behavior of these coatings can be explained if consider that in CeO_2, all valence states of Ce are empty and the system is a wide gap insulator with measured fundamental

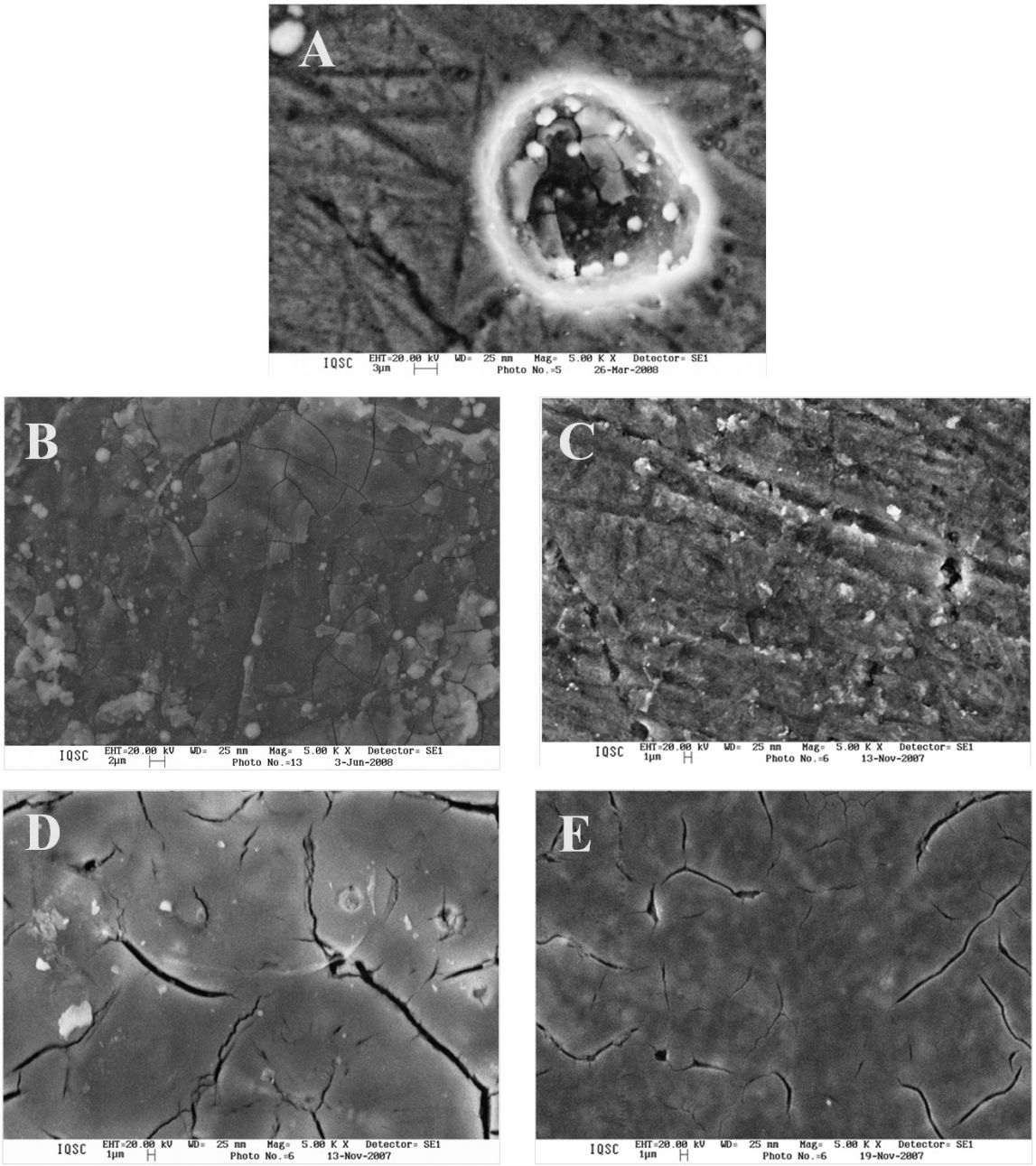

Figure 4. SEM images (5000×) of the AA2024 without deposit (A) and with cerium-based coatings deposited at 100 (B), 200 (C), 300 (D) and 400 °C (E), taken after the polarization experiments represented in Figure 3.

band gap (E_g) of 6.0 eV[31] and with a theoretical band gap of 5.3 eV[32] (determinate using periodic density functional theory calculations).

On the contrary, the micrograph taken at the bare alloy surface after the potentiodynamic polarization experiment (Figure 4A) shows severe corrosion features with the formation of a hole of about 20 µm of diameter. Note that the polarization at bare alloy was carried out only until –0.4 V *versus* SCE that is lower than the 2.0 V *versus* SCE used as limit potential in the polarization experiments carried out with the alloy surfaces covered with cerium oxides.

EIS was also employed to better characterize the protective behavior of the coatings deposited on Al alloy. EIS measurements were carried out using a bare alloy, as well as all the alloy samples protected by Ce-based coatings (Figure 5). The Nyquist plots of the samples with Ce-based anticorrosive coatings presented very high resistances for the charge transfer in the order of gigaohms (*i.e.* about 0.1, 0.14, 0.23 and 0.28 GΩ for coatings synthesized at 100, 200, 300 and 400 °C, respectively). These values of resistance are about three orders of magnitude higher than the corrosion resistance of typical chromate conversion coatings[33] and around five orders of magnitude higher than the observed in the inset of Figure 5 for the bare alloy (*i.e.* ~2.0 kΩ).

The non resolved loops observed at high frequencies can be attributed to both a protective surface film of nanostructured cerium oxide, and to the double layer capacitance at the electrode surface as previously observed for superhydrophobic nanostructured cerium oxide film and fluoroalkylsilane coatings deposited on magnesium alloy in corrosive NaCl aqueous solution[34].

The Nyquist plots of the protected alloys also present intense scattering at low frequencies probably due to the very passive character of the materials; thus, it is non-possible the use of equivalent circuits to fit the experimental impedance spectra.

The electrochemical impedance observed for the protected alloy samples are around five orders of magnitude higher than that showed by the bare alloy corresponding to a tremendous charge resistance. The protective coatings are then non-conductive and could be very efficient for corrosion protection in practical applications.

The corrosive behavior of the bare and protected Al alloys was also tested as a function of the immersion time in corrosive NaCl aqueous solution (3.5%) and the corrosion features were observed by SEM measurements displayed in Figure 6. Extensive superficial corrosion occurred at the alloy without cerium deposits ('bare') after only 10 days of immersion in the saline solution (Figure 6). The corrosion was apparently originated by the presence of intermetallic phases with different electrochemical activities in the alloy; it is due to the presence of holes of sizes in the range 10-50 µm in diameter.

On the other hand, the alloys protected with cerium oxides did not show observable corrosion signals at longer immersion times (30 days). The micrographs taken after immersion test of the protected alloys synthesized using 200, 300 and 400 °C display surfaces with features similar to the observed before immersion (Figure 2). Although the surface of the alloy protected by cerium oxides deposited at 100 °C has different texture than the surface before immersion test, any pitting corrosion was observed and the degradation was minimal. Thus, these results reveal that the sol–gel deposits prepared in this study, at temperatures in the range from 200 to 400 °C, are very efficient against corrosion for long periods of time.

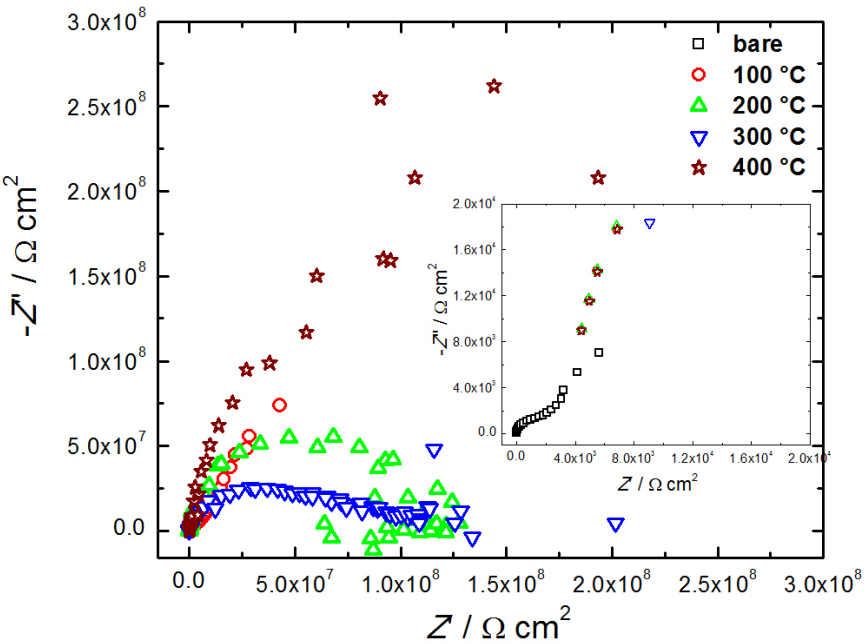

Figure 5. Nyquist plots of the EIS measurements taken on a bare AA2024 substrate and on alloys with sol–gel-based coatings just prepared at 100 °C, 200 °C, 300 °C and at 400 °C. Electrolytes used NaCl 3.5 % solutions. Inset: enlargement of the high frequency region of the plots.

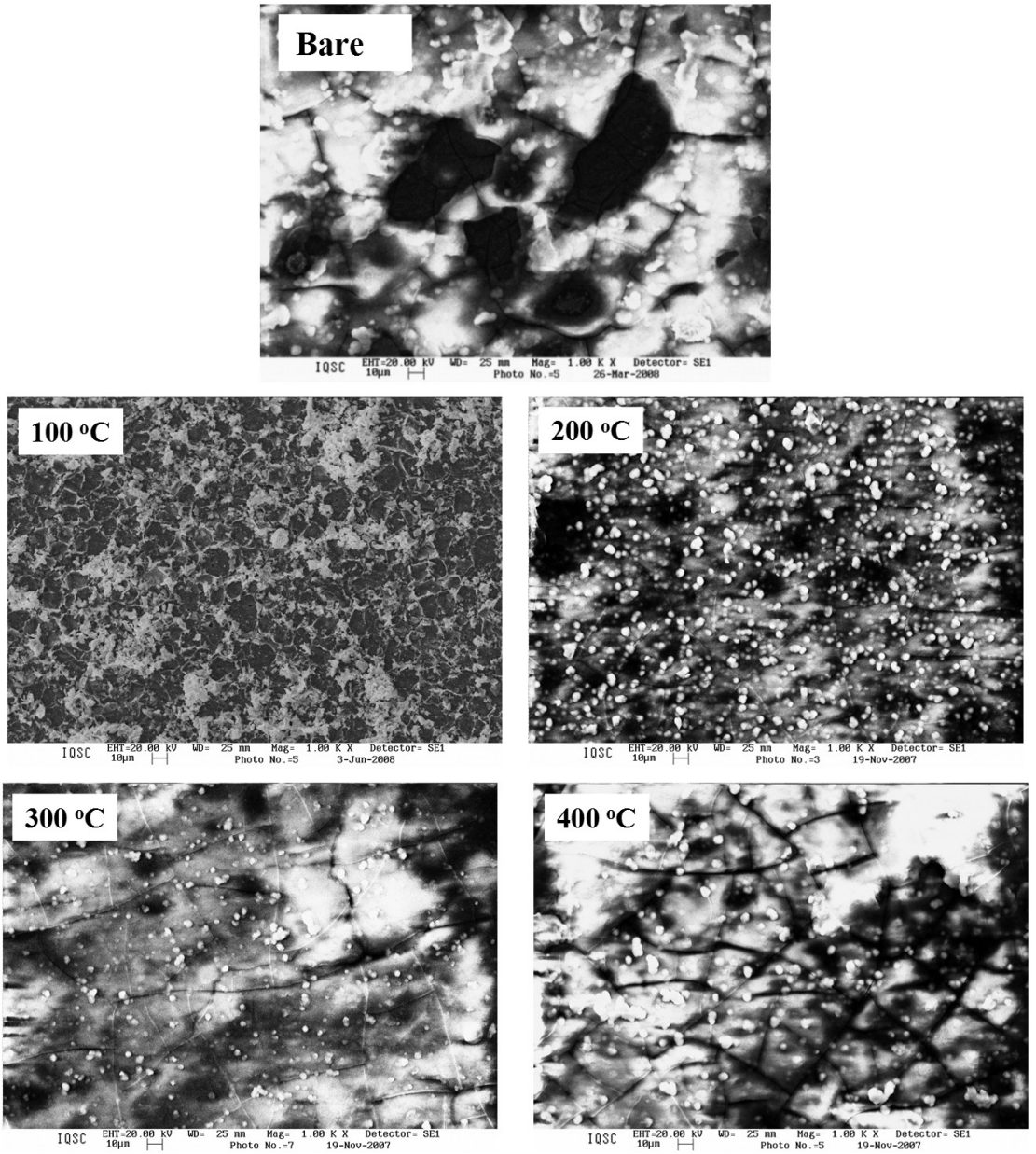

Figure 6. (up) SEM images (1000×) of the AA2024 without deposit and with cerium-based coatings deposited at 100, 200, 300 °C and 400 °C (down), taken after immersion in 3.5 % NaCl solutions by 10 days (AA2024 without deposit) and 30 days (cerium-based coatings).

4. Conclusion

In this study, AA2024 substrates were protected against corrosion using cerium-based sol–gel coatings. The cerium oxides were homogeneously deposited on the electrode surfaces as compact cracked coatings of ceramic aspect when 300 and 400 °C were used in the synthesis. Whereas the use of low calcinations temperatures (100 and 200 °C) yields non uniform coating surfaces with some agglomerates, but without cracks.

The protective coatings prepared using 200, 300 and 400 °C were very resistive and efficient for the passivation of the alloy surfaces and their consequently corrosion protection, even when both, long periods of exposition time to corrosive media, and/or aggressive electrochemical conditions were used. Therefore, the environmentally friendly coatings prepared here by the sol–gel method appear as efficient alternative coatings for the corrosion protection of aluminum alloys and other 'active' alloys or metals.

Acknowledgments

The authors wish to thank the Brazilian Funding Institutions FAPESP (Proc.: 06/50692-2) and CNPq (grants: 303630/2012-4) for the scholarships and financial support.

References

1. Kolics A, Polkinghorne JC, Thomas AE and Wieckowski A. Sorption of sulfate and chloride anions on a well-characterized Al 2024 electrode. *Chemistry of Materials*. 1998; 10:812-824. http://dx.doi.org/10.1021/cm970603i
2. Agency for Toxic Substances and Disease Registry - ATSDR. *Toxicological profile for Chromium (Draft for Public Comment).* Atlanta: U.S. Department of Health and Human Services, Public Health Service; 2009.
3. Zheludkevich ML, Shchukin DG, Yasakau KA, Möhwald H and Ferreira MGS. Anticorrosion coatings with self-healing effect based on nanocontainers impregnated with corrosion inhibitor. *Chemistry of Materials*. 2007; 19:402-411. http://dx.doi.org/10.1021/cm062066k
4. Arnott DR, Hinton BRW and Ryan N. Cationic film-forming inhibitors for the corrosion protection of a 7075 aluminum alloy in chloride solutions. *Materials Performance*. 1987; 26:42-47.
5. Bethencourt M, Botana FJ, Kalvino JJ, Marcos M and Rodriguez-Chacon MA. Lanthanide compounds as environmentally-friendly corrosion inhibitors of aluminium alloys: a review. *Corrosion Science*. 1998; 40:1803-1819. http://dx.doi.org/10.1016/S0010-938X(98)00077-8
6. Arenas MA, Bethencourt M, Botana FJ, de Damborenea J and Marcos M. Inhibition of 5083 aluminium alloy and galvanised steel by lanthanide salts. *Corrosion Science*. 2001; 43:157-170. http://dx.doi.org/10.1016/S0010-938X(00)00051-2
7. Salazar-Banda GR, Moraes SR, Motheo AJ and Machado SAS. Anticorrosive cerium-based coatings prepared by the sol–gel method. *Journal of Sol–Gel Science and Technology*. 2009; 52:415-423. http://dx.doi.org/10.1007/s10971-009-2031-1
8. Yu P, Hayes SA, O'Keefe TJ, O'Keefe MJ and Stoffer JO. The phase stability of cerium species in aqueous systems. *Journal of The Electrochemical Society*. 2006; 153:C74-C79. http://dx.doi.org/10.1149/1.2130572
9. Seah MP. Post-1989 calibration energies for X-ray photoelectron spectrometers and the 1990 Josephson constant. *Surface and Interface Analysis*. 1989; 14:488-488. http://dx.doi.org/10.1002/sia.740140813
10. Wang D and Bierwagen GP. Sol–gel coatings on metals for corrosion protection. *Progress in Organic Coatings*. 2009; 64:327-338. http://dx.doi.org/10.1016/j.porgcoat.2008.08.010
11. Hasannejad H, Aliofkhazraei M, Shanaghi A, Shahrabi T and Sabour AR. Nanostructural and electrochemical characteristics of cerium oxide thin films deposited on AA5083-H321 aluminum alloy substrates by dip immersion and sol–gel methods. *Thin Solid Films*. 2009; 517:4792-4799. http://dx.doi.org/10.1016/j.tsf.2009.03.046
12. Zheludkevich ML, Serra R, Montemor MF, Yasakau KA, Miranda Salvado IM and Ferreira MGS. Nanostructured sol–gel coatings doped with cerium nitrate as pre-treatments for AA2024-T3: Corrosion protection performance. *Electrochimica Acta*. 2005; 51:208-217. http://dx.doi.org/10.1016/j.electacta.2005.04.021
13. Wang H and Akid R. A room temperature cured sol–gel anticorrosion pre-treatment for Al 2024-T3 alloys. *Corrosion Science*. 2007; 49:4491-4503. http://dx.doi.org/10.1016/j.corsci.2007.04.015
14. Moutarlier V, Neveu B and Gigandet MP. Evolution of corrosion protection for sol–gel coatings doped with inorganic inhibitors. *Surface and Coatings Technology*. 2008; 202:2052-2058. http://dx.doi.org/10.1016/j.surfcoat.2007.08.040
15. Verma A, Singh DP, Bakhshi AK and Agnihotry SA. Influence of aging and composition of the precursor sol on the properties of CeO_2-TiO_2 thin films for electrochromic applications. *Journal of Non-Crystalline Solids*. 2005; 351:2501-2512. http://dx.doi.org/10.1016/j.jnoncrysol.2005.07.002
16. Assefa Z, Haire RG, Caulder DL and Shuh DK. Correlation of the oxidation state of cerium in sol–gel glasses as a function of thermal treatment via optical spectroscopy and XANES studies. *Spectrochimica Acta A*. 2004; 60:1873-1881. PMid:15248963. http://dx.doi.org/10.1016/j.saa.2003.10.005
17. He LY and Horiuchi CA. Preparative conversion of oximes to parent carbonyl compounds by cerium(IV) sulfate in acetonitrile and alcohol. *Applied Organometallic Chemistry*. 1999; 13:867-869. http://dx.doi.org/10.1002/(SICI)1099-0739(199912)13:12<867::AID-AOC928>3.0.CO;2-E
18. Chapuzet J-M, Beauchemin S, Daoust B and Lessard J. On the mechanism of alcoholysis of allylic and benzylic alcohols and of epoxides in the presence of ceric ammonium nitrate. *Tetrahedron* 1996; 52:4175-4180. http://dx.doi.org/10.1016/0040-4020(96)00076-2
19. Khalil KMS, Elkabee LA and Murphy B. Formation and characterization of different ceria/silica composite materials via dispersion of ceria gel or soluble ceria precursors in silica sols. *Journal of Colloid and Interface Science*. 2005; 287:534-541. PMid:15925620. http://dx.doi.org/10.1016/j.jcis.2005.02.041
20. De Oliveira-Sousa A, Da Silva MAS, Machado SAS, Avaca LA and De Lima-Neto P. Influence of the preparation method on the morphological and electrochemical properties of Ti/IrO_2-coated electrode. *Electrochimica Acta*. 2000; 45:4467-4473. http://dx.doi.org/10.1016/S0013-4686(00)00508-9
21. Panić VV and Nikolić BŽ. Sol–gel prepared active ternary oxide coating on titanium in cathodic protection. *Journal of the Serbian Chemical Society*. 2007; 72:1393-1402. http://dx.doi.org/10.2298/JSC0712393P
22. Jara CC, Salazar-Banda GR, Arratia RS, Campino JS and Aguilera MI. Improving the stability of Sb doped Sn oxides electrode thermally synthesized by using an acid ionic liquid as solvent. *Chemical Engineering Journal*. 2011; 171:1253-1262. http://dx.doi.org/10.1016/j.cej.2011.05.039
23. Sayilkan H, Sener S, Sener E and Sülü M. The sol–gel synthesis and application of some anticorrosive coating materials. *Materials Science*. 2003; 39:733-739. http://dx.doi.org/10.1023/B:MASC.0000023514.74970.73
24. Joshua Du Y, Damron M, Tang G, Zheng H, Chu CJ and Osborne JH. Inorganic/organic hybrid coatings for aircraft aluminum alloy substrates. *Progress in Organic Coatings*. 2001; 41:226-232. http://dx.doi.org/10.1016/S0300-9440(01)00133-3
25. Ballard RL, Williams JP, Njus JM, Kiland BR and Soucek MD. Inorganic-organic hybrid coatings with mixed metal oxides. *European Polymer Journal*. 2001; 37:381-398. http://dx.doi.org/10.1016/S0014-3057(00)00105-1
26. Wang Z-L and Zeng R-C. Comparison in characterization of composite and sol–gel coating on AZ31 magnesium alloy. *Transactions of Nonferrous Metals Society of China*. 2010; 20:s665-s669. http://dx.doi.org/10.1016/S1003-6326(10)60558-4
27. Naval Air Warfare Center. Aircraft Division. *Military Specification*: Anodic Coatings for Aluminum and Aluminum Alloys. Naval Air Warfare Center, Aircraft Division; 2003.
28. Karpagam V, Sathiyanarayanan S and Venkatachari G. Studies on corrosion protection of Al2024 T6 alloy by electropolymerized polyaniline coating. *Current Applied Physics*. 2008; 8:93-98. http://dx.doi.org/10.1016/j.cap.2007.05.005
29. Zubillaga O, Cano FJ, Azkarate I, Molchan IS, Thompson GE and Skeldon P. *Surface and Coatings Technology*. 2009; 203:1494-1501. http://dx.doi.org/10.1016/j.surfcoat.2008.11.023

30. Shabani-Nooshabadi M, Ghoreishi SM and Behpour M. Electropolymerized polyaniline coatings on aluminum alloy 3004 and their corrosion protection performance. Electrochimica Acta 2009; 54:6989-6995. http://dx.doi.org/10.1016/j.electacta.2009.07.017

31. Wuilloud E, Delley B, Schneider W-D and Baer Y. Spectroscopic evidence for localized and extended *f*-symmetry states in CeO_2. *Physical Review Letters*. 1984; 53:202-205. http://dx.doi.org/10.1103/PhysRevLett.53.202

32. Da Silva JLF, Ganduglia-Pirovano MV, Sauer J, Bayer V and Kresse G. Hybrid functionals applied to rare-earth oxides: The example of ceria. *Physical Review B*. 2007; 75:045121-1-045121-10.

33. Buchheit RG, Mamidipally SB, Schmutz P and Guan H. Active corrosion protection in Ce-modified hydrotalcite conversion coatings. *Corrosion*. 2002; 58:3-14. http://dx.doi.org/10.5006/1.3277303

34. Ishizaki T, Masuda Y and Sakamoto M. Corrosion resistance and durability of superhydrophobic surface formed on magnesium alloy coated with nanostructured cerium oxide film and fluoroalkylsilane molecules in corrosive NaCl aqueous solution. *Langmuir*. 2011; 27:4780-4788. PMid:21417352. http://dx.doi.org/10.1021/la2002783